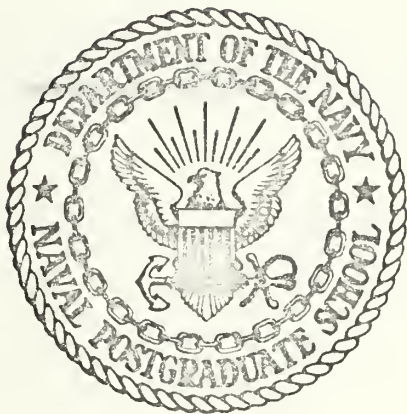


SLOT LINE FERRITE ISOLATOR

Imon Lester Pilcher

NAVAL POSTGRADUATE SCHOOL

Monterey, California



THESIS

SLOT LINE FERRITE ISOLATOR

by

Imon Lester Pilcher

Thesis Advisor:

J.B. Knorr

June 1973

T355161

Approved for public release; distribution unlimited.

Slot Line Ferrite Isolator

by

Imon Lester Pilcher
Lieutenant, United States Navy
B.S.E.E., University of Washington, 1964

Submitted in partial fulfillment of the
requirements for the degree of

MASTER OF SCIENCE IN ELECTRICAL ENGINEERING

from the

NAVAL POSTGRADUATE SCHOOL

June 1973

ABSTRACT

A slot line isolator configuration is investigated experimentally. The configuration is analyzed using perturbation theory. Theoretical results obtained from a computer program based on the analysis are compared with the experimental measurements.

TABLE OF CONTENTS

I.	INTRODUCTION -----	8
II.	MICROWAVE FERRITES -----	9
III.	SLOT LINE ISOLATOR THEORY -----	12
IV.	SLOT LINE ISOLATOR -----	17
	A. EXPERIMENT PROCEDURE AND SET UP -----	17
	B. EXPERIMENTAL RESULTS -----	22
	1. Resonant Field -----	22
	2. Forward and Reverse Loss Measurements --	22
V.	CONCLUSIONS -----	36
APPENDIX A:	RESULTS OF INTEGRATION OF MODIFIED BESSEL FUNCTIONS FOR SMALL VALUES OF τ_a -----	37
COMPUTER PROGRAM	-----	40
LIST OF REFERENCES	-----	42
INITIAL DISTRIBUTION LIST	-----	43
FORM DD 1473	-----	44

LIST OF TABLES

TABLE

I	Slot line parameters for substrate thickness of 0.125 inches and $\epsilon_r = 16.0$ -----	15
II	Representative values of the integration of the modified Bessel functions for different ferrite slab positions -----	16
III	Ferrite microwave characteristics -----	19
IV	Comparison of theoretical and experimental values of external field for maximum reverse loss at 3 GHz -----	22

LIST OF ILLUSTRATIONS

Figure

1.	Electron precession about a static magnetic field with a superimposed r.f. field alternating at the same frequency -----	9
2.	Slot line isolator configuration -----	12
3.	Slot line isolator in the experimental configuration -----	18
4.	Block diagram of the testing circuit for forward and reverse attenuation -----	19
5.	Tensor susceptibility component X'_{xx} for Garnet and Spinel -----	20
6.	Tensor susceptibility component X'_{xy} for Garnet and Spinel -----	21
7.	Forward attenuation for Garnet $a = 0.125$ inches -----	23
8.	Forward attenuation for Garnet $a = 0.075$ inches -----	24
9.	Reverse attenuation for Garnet $a = 0.125$ inches -----	25
10.	Reverse attenuation for Garnet $a = 0.075$ inches -----	26
11.	Forward attenuation for Spinel $a = 0.050$ inches -----	27
12.	Forward attenuation for Spinel $a = 0.025$ inches -----	28
13.	Reverse attenuation for Spinel $a = 0.050$ inches -----	29
14.	Reverse attenuation for Spinel $a = 0.025$ inches -----	30
15.	Theoretical and experimental values of reverse loss at the center frequency as a function of distance from the center of the slot for Garnet -----	32

Figure

16.	Theoretical and experimental values of reverse loss at the center frequency as a function of distance from the center of the slot for Spinel -----	33
17.	Ratio of reverse to forward attenuation at the center frequency as a function of distance from the center of the slot for Garnet -----	34
18.	Ratio of reverse to forward attenuation at center frequency as a function of distance from the center of the slot for Spinel -----	35

ACKNOWLEDGEMENT

The author wishes to thank Professor J. B. Knorr who suggested the topic, developed the theory and who gave invaluable assistance during the course of this work. A special tribute of gratitude goes to my wife and children, whose love and patience during this educational endeavor are something for which the author shall be eternally grateful.

I. INTRODUCTION

The slot line has gained importance as a transmission line in microwave systems. The field distribution of this line has been investigated by Cohn [1]. This investigation revealed that the slot line has areas of elliptical polarization of the field on both the air and substrate sides of the metal conductor. Because of this elliptical polarization, non-reciprocal propagation due to interaction with ferrite material is possible. A ferrite device for non-reciprocal modes of propagation has been presented by Hines [2] for a strip line. Thus the development of a non-reciprocal device for a slot is initiated.

The ferrite slot line isolator is developed from the theory of microwave ferrites and slot line wave propagation on a dielectric substrate. Quantitative treatments are derived from wave guide perturbation theory as applied to open boundary structures supporting bound waves and the application of this perturbation theory to a slot line loaded with a ferrite slab.

The purpose of this thesis is to apply the theoretical analysis of the slot line isolator to a practical isolator and to compare the experimental and theoretical results. The investigation of two types of ferrites placed on the slot line at selected locations will be included in the experimental results.

II. MICROWAVE FERRITES

The permeability of a ferrite exhibits a tensor quality at microwave frequencies. It is the off-diagonal elements, which are of opposite sign and are imaginary, of the tensor that produce the non-reciprocal effects of the ferrite. The permeability tensor, $[\chi]$, can be derived from the equations of motion using the simple electron model shown in Figure 1.

When a static external magnetic field (\overline{H}_0) is applied to a ferrite material the magnetic dipole moment ($\overline{\mu}$) will precess about an internal magnetic field (\overline{H}_i).

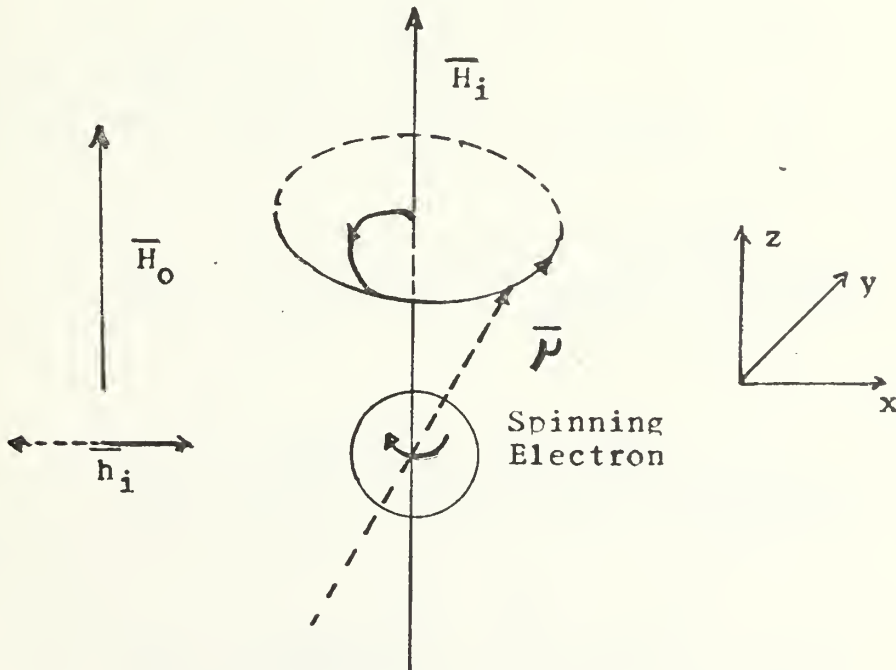


Figure 1. Electron precession about a static magnetic field with a superimposed r.f. field alternating at the same frequency.

The frequency of this precession of (f_o) is dependent upon the value of \overline{H}_1 . A damping factor (α) will cause the magnitude of the precession to decay until $\overline{\mu}$ comes into alignment with \overline{H}_1 . If a small magnetic r. f. field (\overline{h}_1) is applied transverse to \overline{H}_1 and its frequency (f) is synchronous with f_o , the magnitude of precession will increase and energy can be absorbed from the r. f. signal.

The derivation of the permeability tensor $[\chi]$ may be found in references [3] and [4]. The results are shown below:

$$[\chi] = \begin{bmatrix} X_{xx} & X_{xy} & 0 \\ X_{xy} & X_{yy} & 0 \\ 0 & 0 & 0 \end{bmatrix} \quad (1)$$

where $X_{xx} = X_{yy}$ and $X_{xy} = -X_{yx}$.

The real and imaginary parts of $[\chi]$ are

$$X'_{xx} = \frac{f_m f_o (f_o^2 - f^2) + f_m f_o f^2 \alpha^2}{[f_o^2 - f^2(1 + \alpha^2)]^2 + 4f_o^2 f^2 \alpha^2} \quad (2)$$

$$X''_{xx} = \frac{f_m f \alpha (f_o^2 + f^2(1 + \alpha^2))}{[f_o^2 - f^2(1 + \alpha^2)]^2 + 4f_o^2 f^2 \alpha^2} \quad (3)$$

$$X'_{xy} = \frac{-j f_m f (f_o^2 - f^2(1 + \alpha^2))}{[f_o^2 - f^2(1 + \alpha^2)]^2 + 4f_o^2 f^2 \alpha^2} \quad (4)$$

$$X'_{xy} = \frac{-j2f_m f_o f^2 \alpha}{[f_o^2 - f^2(1 + \alpha^2)]^2 + 4f_o^2 f^2 \alpha^2} \quad (5)$$

where $f_m = 4\pi M_s \gamma$ and $f_o = \gamma H_i$ (6), (7)

with $\gamma \simeq 2.8(\text{MH}_z/\text{OERSTED})$ and M_s = saturation magnetization.

The line width (ΔH) of the ferrite determines the damping factor of Equations (2) - (5). Thus α is given by

$$\omega \alpha = \frac{\gamma \Delta H}{2} \quad (8)$$

The magnetic field H_i in the ferrite slab of Figure 2 is approximately

$$H_i \simeq H_o - 4\pi M_s \quad (9)$$

where H_o is the field in the medium surrounding the ferrite and $H_o > 4\pi M_s$.

III. SLOT LINE ISOLATOR THEORY

The slot line r. f. magnetic fields are elliptically polarized in the x,y plane and the fields are tightly bound to the substrate [5]. This suggests that a ferrite slab with its broad face perpendicular to the z-axis would be an appropriate geometry for interaction between the magnetized ferrite and the slot field. This configuration is shown in Figure 2.

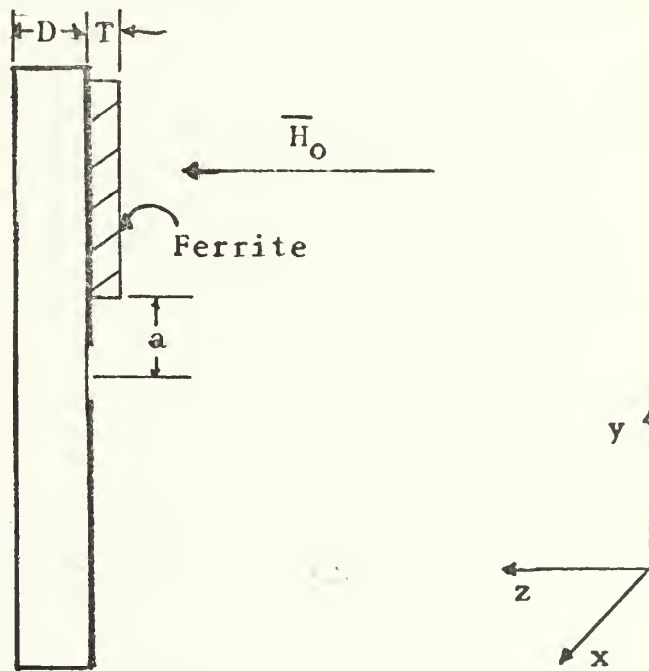


Figure 2. Slot line isolator configuration.

Perturbation theory as applied to an open boundary structure supporting a bound wave can now be considered for the geometry of Figure 2. The change in the propagation

constant due to a small change in the type of material in the vicinity of a guiding structure such as a slot line is given by Knorr [6].

$$(\Gamma' + \Gamma^*) = \frac{j\omega \int_S (\epsilon_0 [\Delta\chi_e] \cdot \bar{E}' \cdot \bar{E}^* + \mu_0 [\Delta\chi_m] \cdot \bar{H} \cdot \bar{H}^*) da}{\int_S (\bar{E}^* \times \bar{H}' + \bar{E} \times \bar{H}^*) \cdot \bar{a}_z da} \quad (10)$$

where

$$[\Delta\chi_e] = (\epsilon_r - 1)[1]$$

and

$$[\Delta\chi_m] = \begin{bmatrix} X_{xx} & X_{xy} & 0 \\ -X_{xy} & X_{xx} & 0 \\ 0 & 0 & 0 \end{bmatrix}$$

also

$$\bar{E}' = (E_z / \epsilon_r) \bar{a}_z \quad \bar{H} = \bar{H}'$$

The primed quantities refer to perturbed values.

The field in the region to be occupied by the ferrite slab are given approximately by [7]

$$H_x = \frac{j\pi V_0}{\eta\lambda} [(\lambda/\lambda')^2 - 1] [jH_0^{(1)}(k_c y)] \quad (11)$$

$$H_y = \pm \frac{V_o}{\eta \lambda'} (\lambda/\lambda') \sqrt{(\lambda/\lambda')^2 - 1} [-H_1^{(1)}(k_c y)] \quad (12)$$

$$E_z = -\frac{V_o \pi}{\lambda} \sqrt{(\lambda/\lambda')^2 - 1} [-H_1^{(1)}(k_c y)] \quad (13)$$

Upon substituting Equations (11) - (13) in Equation (10), the real part of the propagation constant for a forward or reverse traveling wave is found to be [8].

$$\begin{aligned} \alpha_{\pm} = & 2(Z_o/\eta)(T/\lambda)(1/\lambda)\{\chi_{xx}'[(\lambda/\lambda')^2 - 1]^{\frac{3}{2}} I_o(\tau_a) \\ & + (\lambda/\lambda')^2[(\lambda/\lambda')^2 - 1]^{\frac{1}{2}} I_1(\tau_a)) \\ & 2(j\chi_{xy}'(\lambda/\lambda')^2[(\lambda/\lambda')^2 - 1] I_{01}(\tau_a) \end{aligned} \quad (14)$$

where

$$I_o(\tau_a) = \int_{\tau_a}^{\infty} K_o^2(x) dx \quad (15)$$

$$I_1(\tau_a) = \int_{\tau_a}^{\infty} K_1^2(x) dx \quad (16)$$

$$I_{01}(\tau_a) = \int_{\tau_a}^{\infty} K_o(x)K_1(x) dx = \frac{1}{2}K_o^2(\tau_a) \quad (17)$$

$$\tau = 2\pi/\lambda[(\lambda/\lambda')^2 - 1]^{\frac{1}{2}} \quad (18)$$

The numerical values of the integrals (15) - (17) were found using two subroutines, BESK and QTFE, that are available as part of the System/360 Scientific Subroutine Package [9].

The slot line characteristics used in computing α were acquired from the impedance and slot line wave length graphs of [7]. These values are given in Table I for the slot line isolator manufactured for this thesis. Representative values of the integration of the modified Bessel functions by the trapezoidal rule (second order formula) are given in Table II. Graphs of these integrals for small values of τ_a are shown in Appendix A.

TABLE I

Slot line parameters for substrate thickness of 0.125 inches and $\epsilon_r = 16.0$.

FREQUENCY (GHz)	λ' (cm)	Z_0 (OHMS)	τ (cm ⁻¹)
2.0	6.00	71	0.952
2.25	5.25	72	1.11
2.5	4.68	73	1.24
2.75	4.23	75	1.37
3.0	3.83	76	1.52
3.25	3.50	76	1.66
3.5	3.2	76	1.83
3.75	2.95	77	1.98
4.0	2.76	77	2.12

TABLE II

Representative values of the integration of the modified Bessel functions for different ferrite slab positions.

a = 0.125 inches			
FREQUENCY (GHz)	$I_0(\tau a)$	$I_1(\tau a)$	$I_{01}(\tau a)$
2.0	0.53	1.60	0.92
2.25	0.44	1.30	0.76
2.50	0.39	1.00	0.64
2.75	0.34	0.80	0.54
3.0	0.28	0.65	0.45
3.25	0.25	0.55	0.39
3.5	0.21	0.45	0.32
3.75	0.18	0.35	0.27
4.0	0.16	0.30	0.24
a = 0.050 inches			
2.0	1.10	6.0	2.47
2.25	0.97	4.8	2.18
2.50	0.93	4.2	1.96
2.75	0.88	3.8	1.78
3.0	0.80	3.2	1.60
3.25	0.74	2.8	1.44
3.5	0.68	2.4	1.28
3.75	0.63	2.1	1.16
4.0	0.58	1.9	1.07

IV. SLOT LINE ISOLATOR

A. EXPERIMENTAL PROCEDURE AND SET UP

The slot line used for the isolator was constructed from copper clad $\epsilon_r = 16$, one-eighth inch thick substrate. The isolator was designed to operate at a center frequency of 3 GHz and to match a 50 ohm coaxial cable (0.141 inch O.D. semi-rigid) thru a slot line to coaxial transition. Figure 3 shows the slot line isolator manufactured and tested for this thesis. The isolator is shown in the testing position. The static magnetic field was perpendicular to the broad face of the slot line. The isolator was mounted in a non-ferrous retainer and the ferrite slab was held in place by non-ferrous clamps.

The isolator was positioned for testing between the pole pieces of an electromagnet with a range of 0 to 4000 Gauss for a 2 inch gap. The circuit set up for taking measurements is shown in Figure 4.

Because the current in the electromagnet could not be reversed, measurements for forward and reverse loss were made by exchanging the inlet and the outlet coaxial cables. The experimental measurements were performed so that data reflected loss due only to the ferrite slab.

Two types of microwave ferrite materials were investigated and their characteristics are given in Table III. The program listed on page 40 computes the imaginary parts

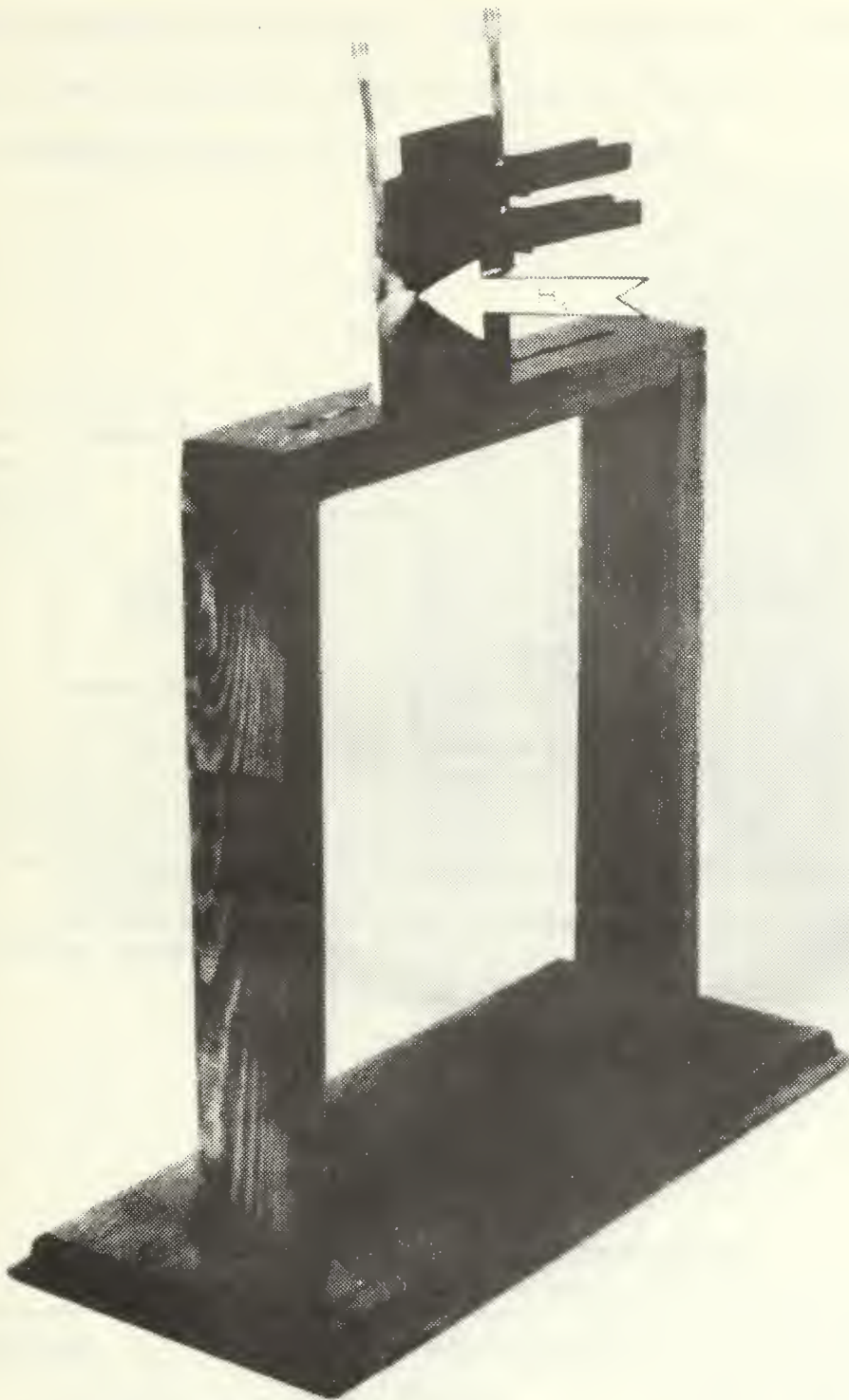


Figure 3. Slot line isolator in the experimental configuration.

of the susceptibility tensor for both materials and the results are plotted in Figures 5 and 6. These two materials were selected because of their availability.

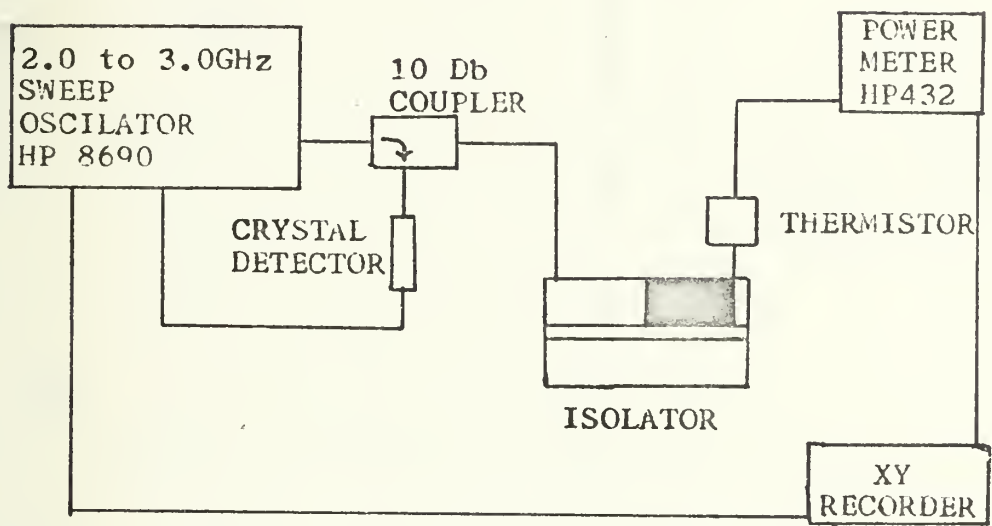


Figure 4. Block diagram of the testing circuit for forward and reverse attenuation.

TABLE III

Ferrite Microwave Characteristics

MATERIAL	SATURATION MAGNETIZATION $4\pi M_s$ (GAUSS)	LINE WIDTH $\Delta H(-3\text{Db})$	f_m (GHz)
SPINEL	1750	225	4.80
GARNET	1200	75	3.39

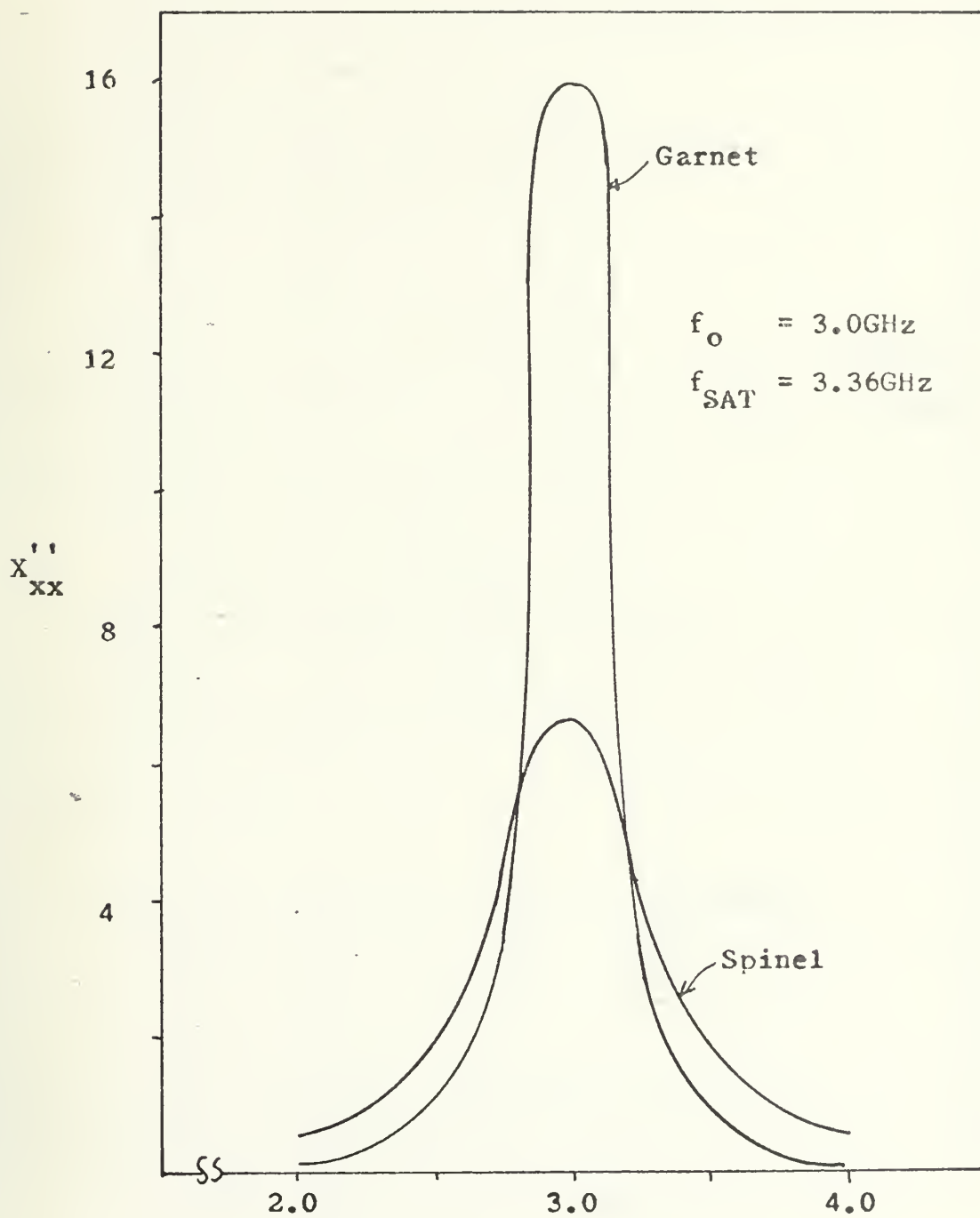


Figure 5. Tensor susceptibility component X''_{xx} for Garnet and Spinel.

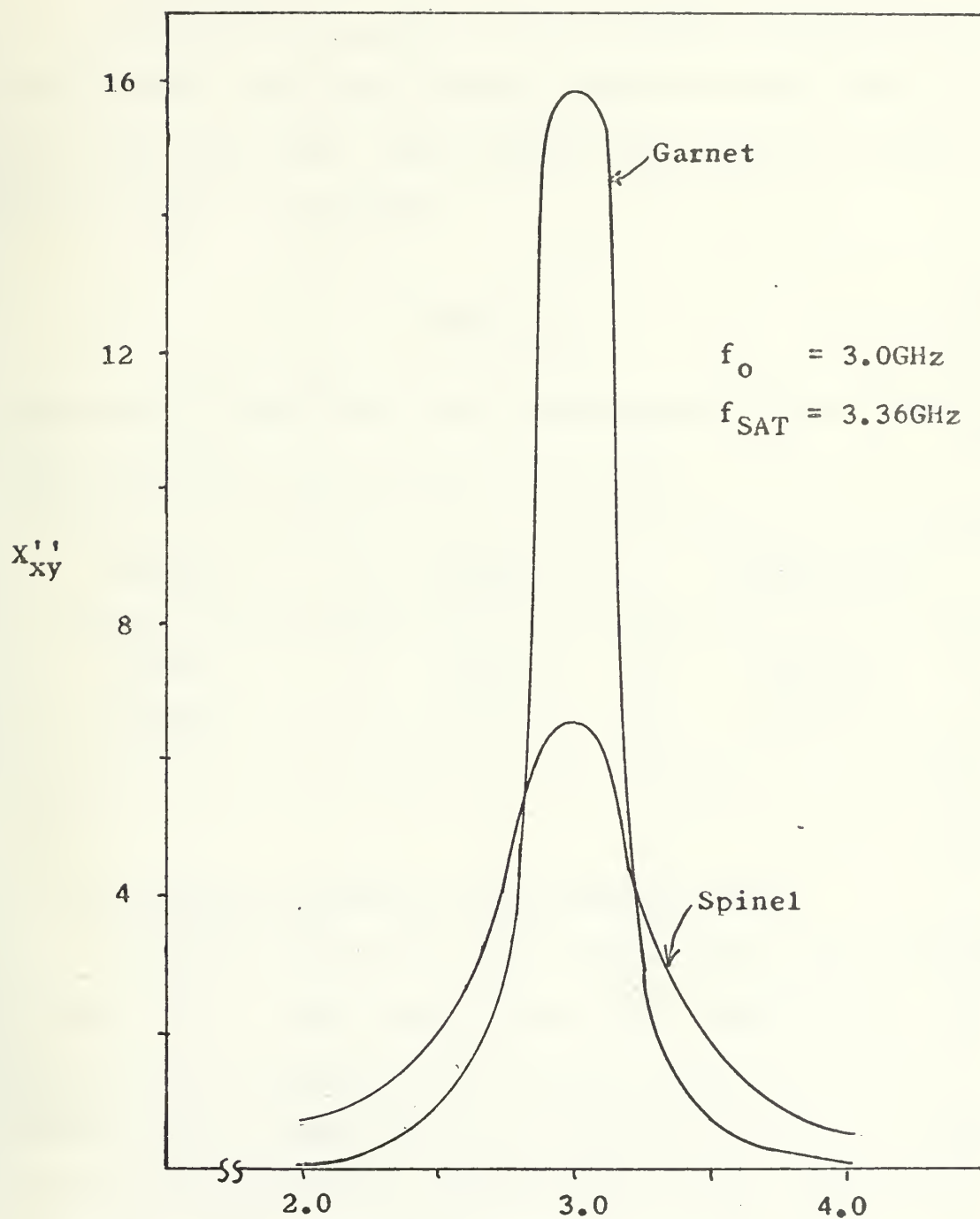


Figure 6. Tensor susceptibility component X''_{xy} for Garnet and Spinel.

B. EXPERIMENTAL RESULTS

1. Resonant Field

The first property of the isolator investigated was the magnetic field that produced maximum reverse loss at the center frequency. The results are compared in Table IV for the two ferrite slabs.

TABLE IV

Comparison of theoretical and experimental values of external field for maximum reverse loss at 3 GHz.

MATERIAL	THEORETICAL	EXPERIMENTAL
SPINEL	2830 G	2500 G
GARNET	2280 G	2125 G

2. Forward and Reverse Loss Measurements

Forward and reverse loss measurements were conducted at four ferrite slab positions and were compared with theoretical values computed by the program found on page 40. Figures 7 and 8 show results of forward loss for the Garnet for two slab positions, Figures 9 and 10 show the results of the reverse attenuation for the same ferrite positions. Similar graphs were plotted for the Spinel, which has a larger band width (ΔH). These results are shown on Figures 11 thru 14.

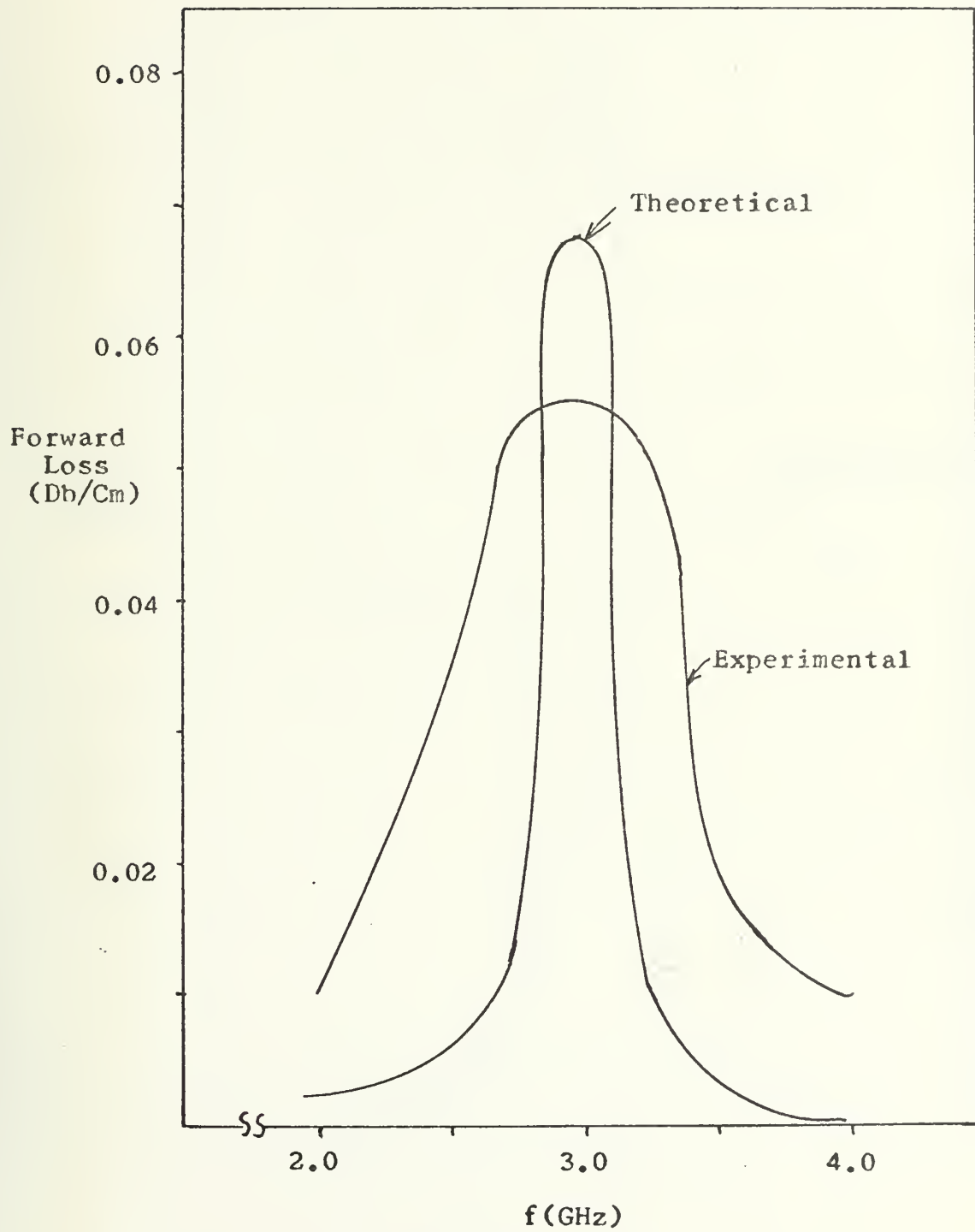


Figure 7. Forward Attenuation for Garnet $a = 0.125$ inches.

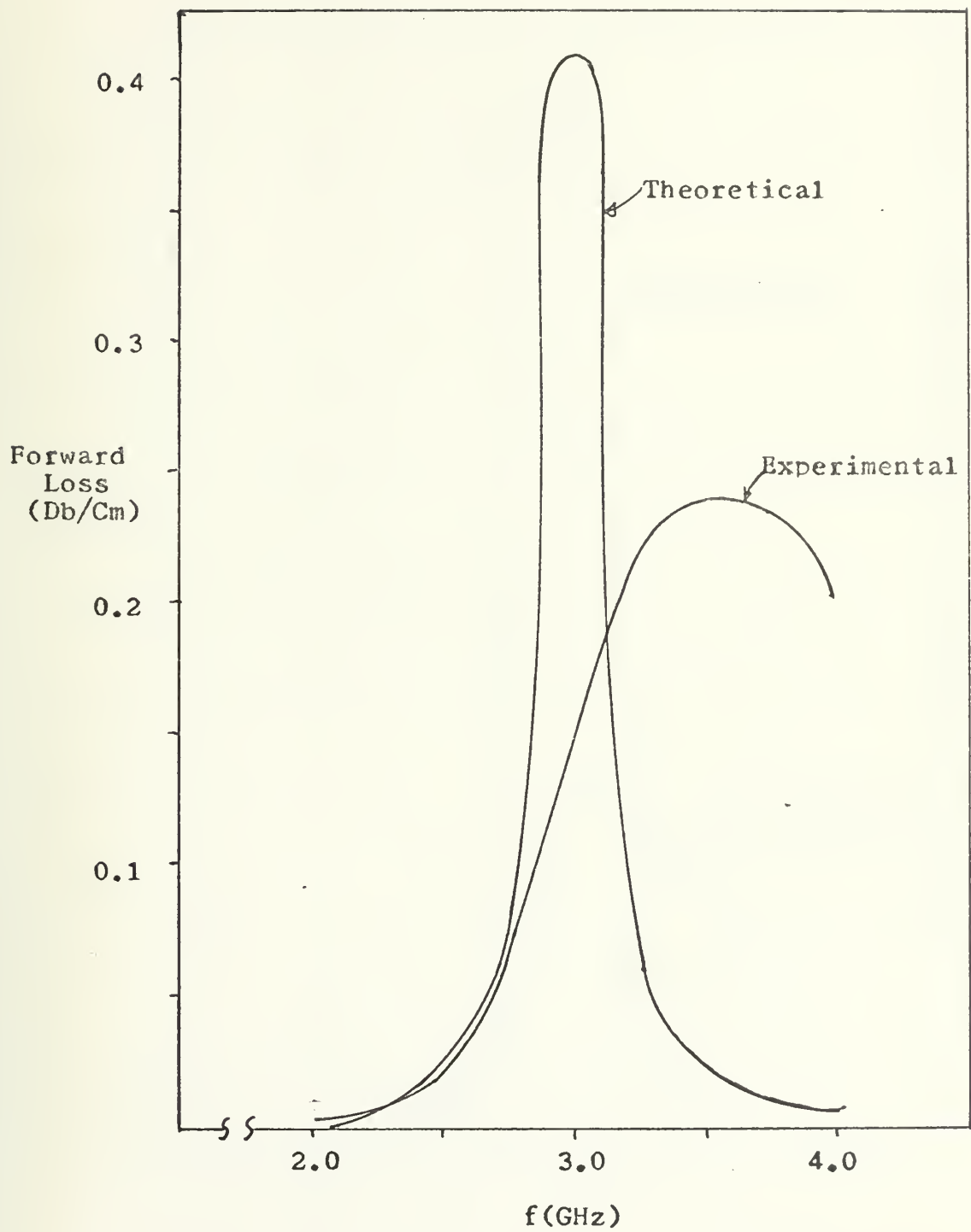


Figure 8. Forward attenuation for Garnet $a = 0.075$ inches.

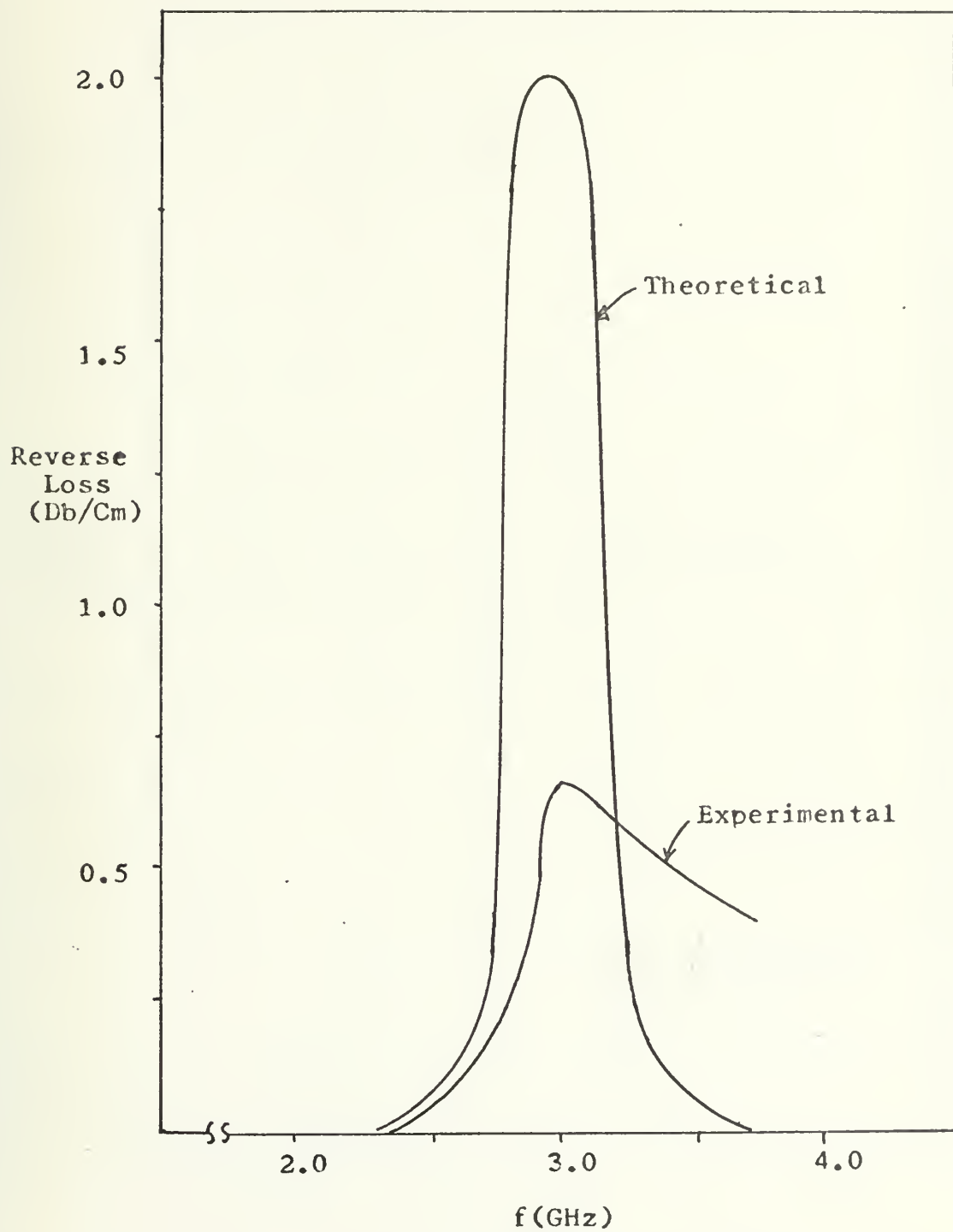


Figure 9. Reverse attenuation for Garnet $a = 0.125$ inches.

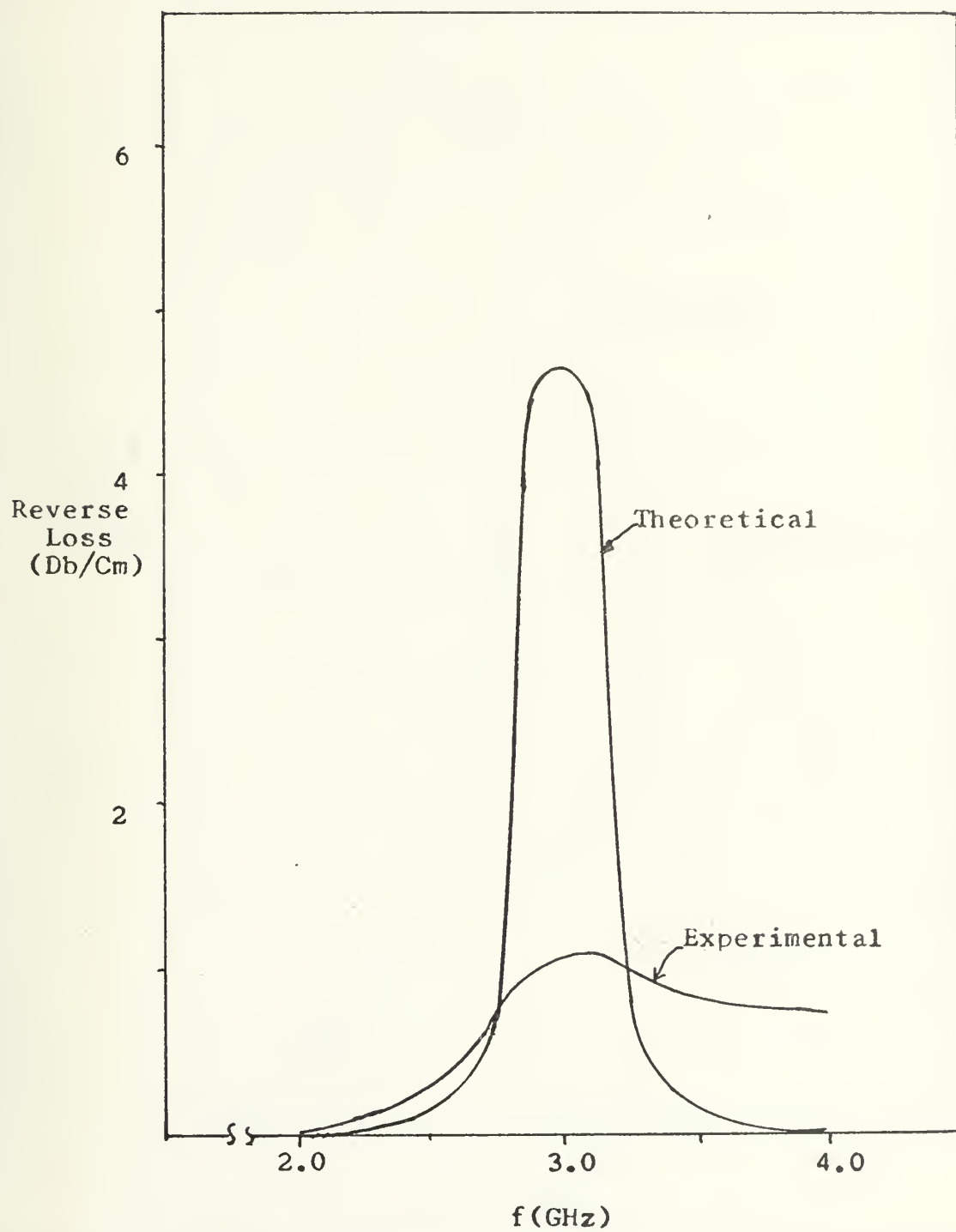


Figure 10. Reverse attenuation for Garnet $a = 0.075$ inches.

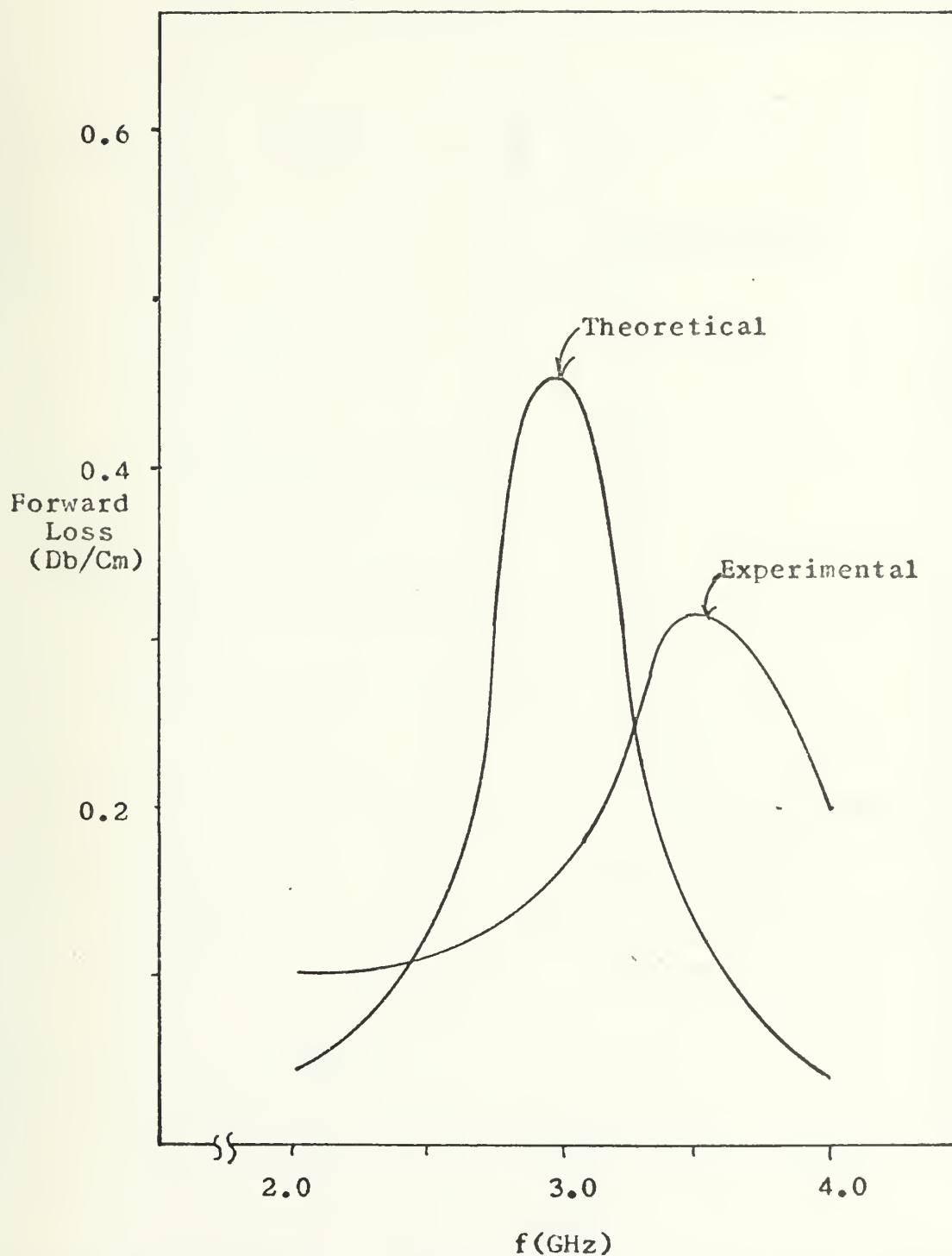


Figure 11. Forward attenuation for Spinel $a = 0.050$ inches.

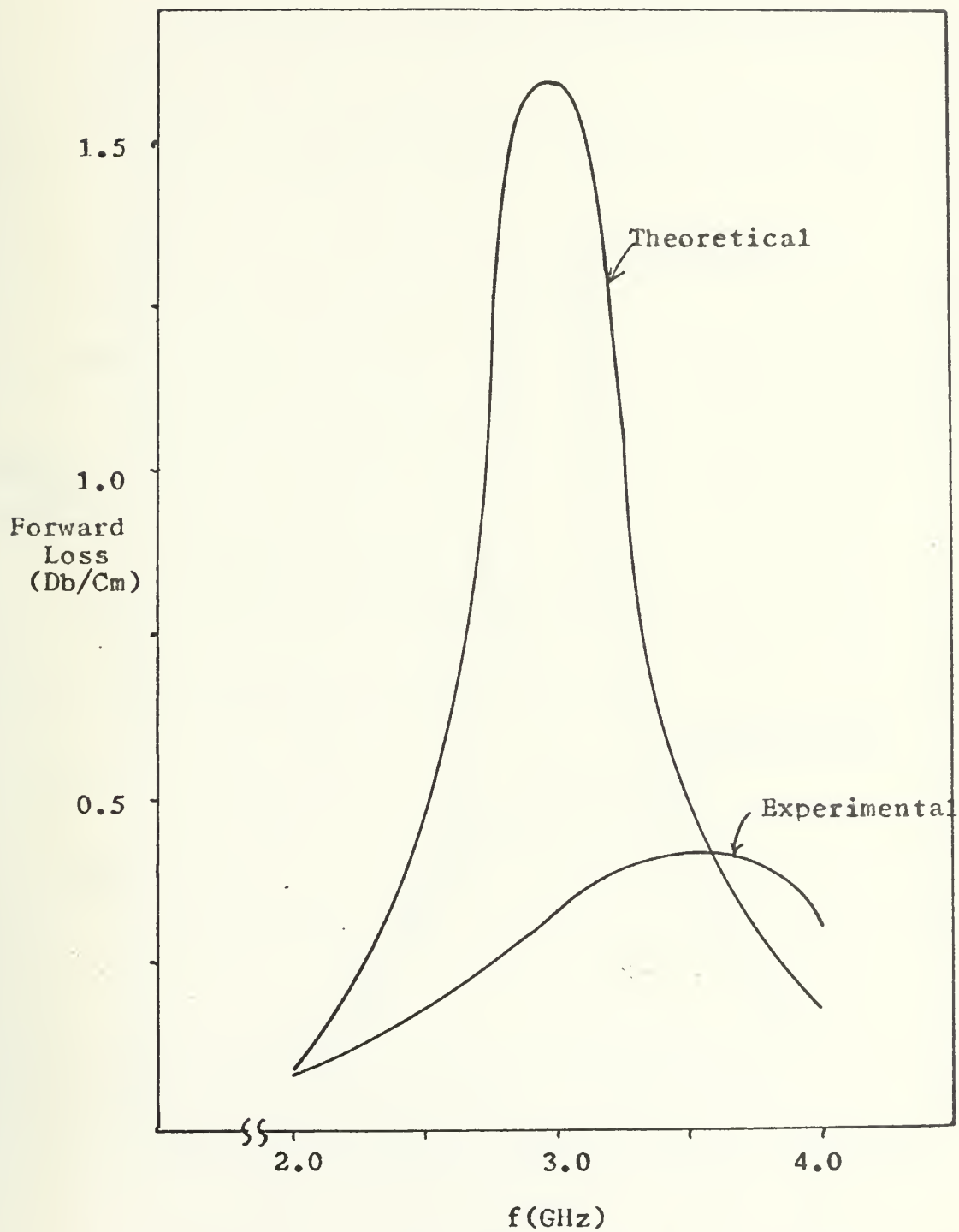


Figure 12. Forward attenuation for Spinel $a = 0.025$ inches.

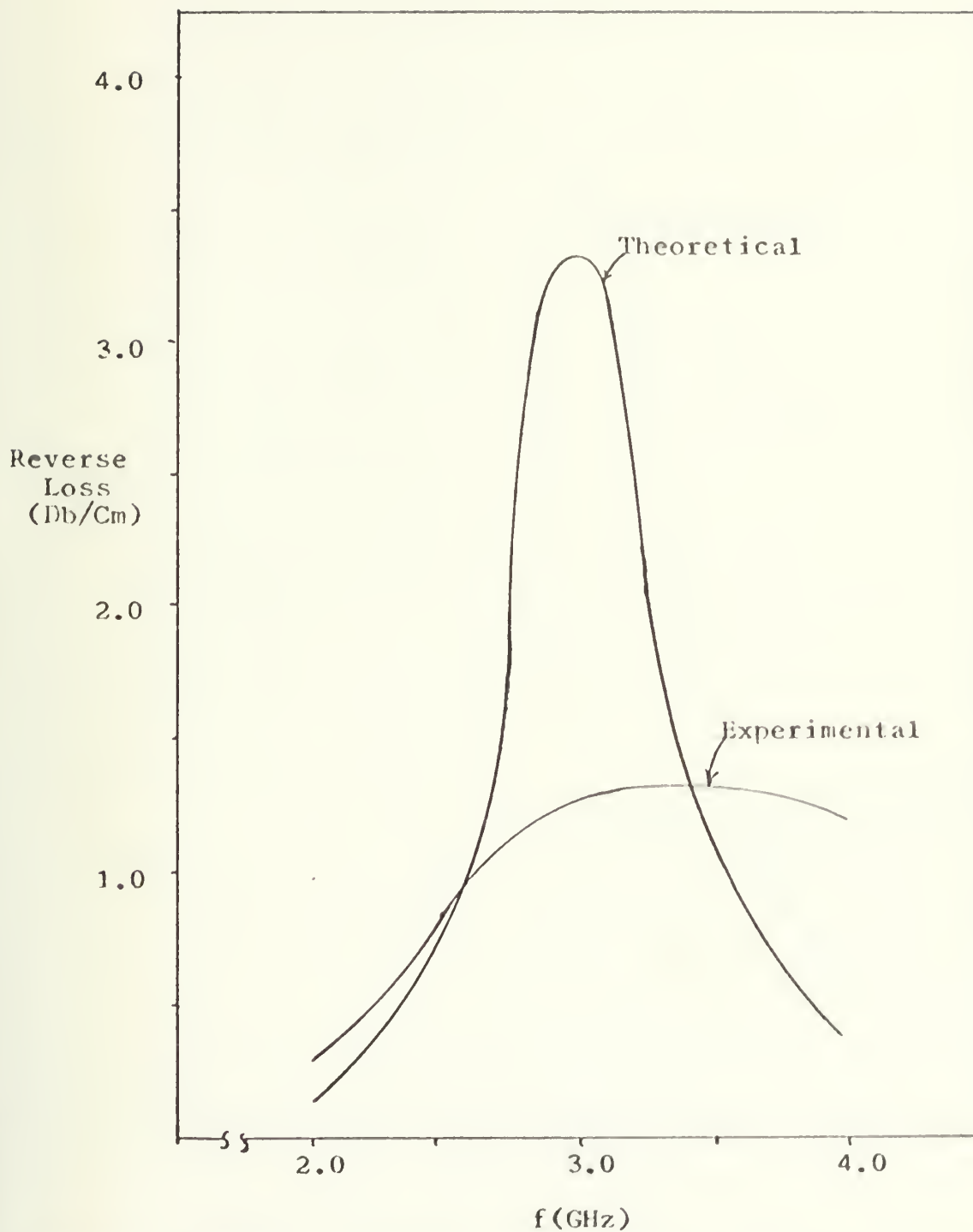


Figure 13. Reverse attenuation for Spinel $a = 0.050$ inches.

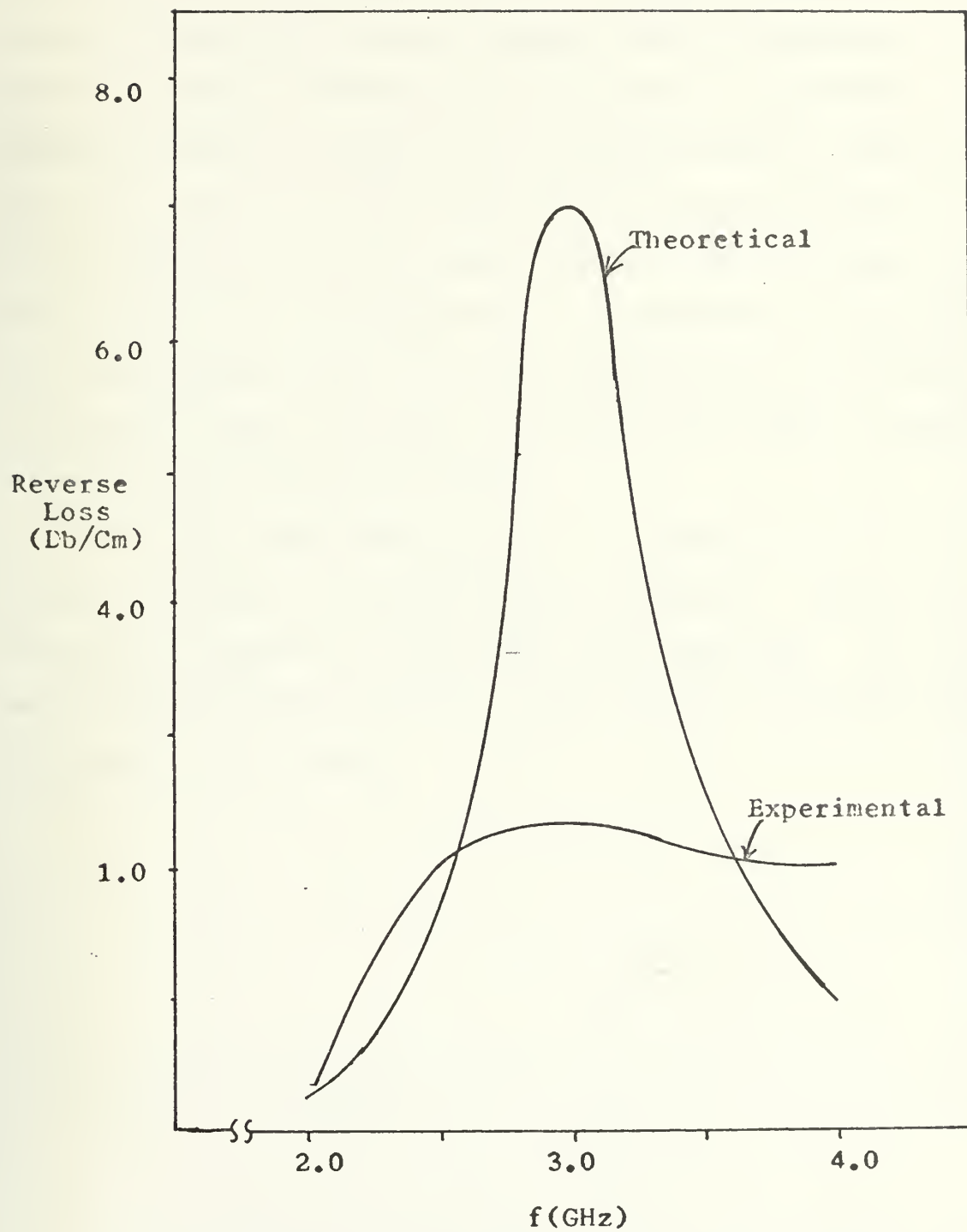


Figure 14. Reverse attenuation for Spinel $a = 0.025$ inches.

The results indicate that the experimental values agreed qualitatively with theory but in all cases theory predicted greater forward and reverse losses. This discrepancy partially can be attributed to the error in the Hankel-Function solution to the slot line field near the center of the slot. Also the effective area of contact between the ferrite and the slot line was somewhat reduced because of a warp in the slot line substrate. A comparison of theoretical and experimental values of reverse attenuation as a function of distance from the center of the slot are shown in Figures 15 and 16 for Garnet and Spinel.

One of the specifications for an isolator is that the ratio of reverse to forward loss be maximized. This ratio is shown on Figures 17 and 18 for both materials. As can be seen this ratio increases as the ferrite is moved toward the center of the slot.

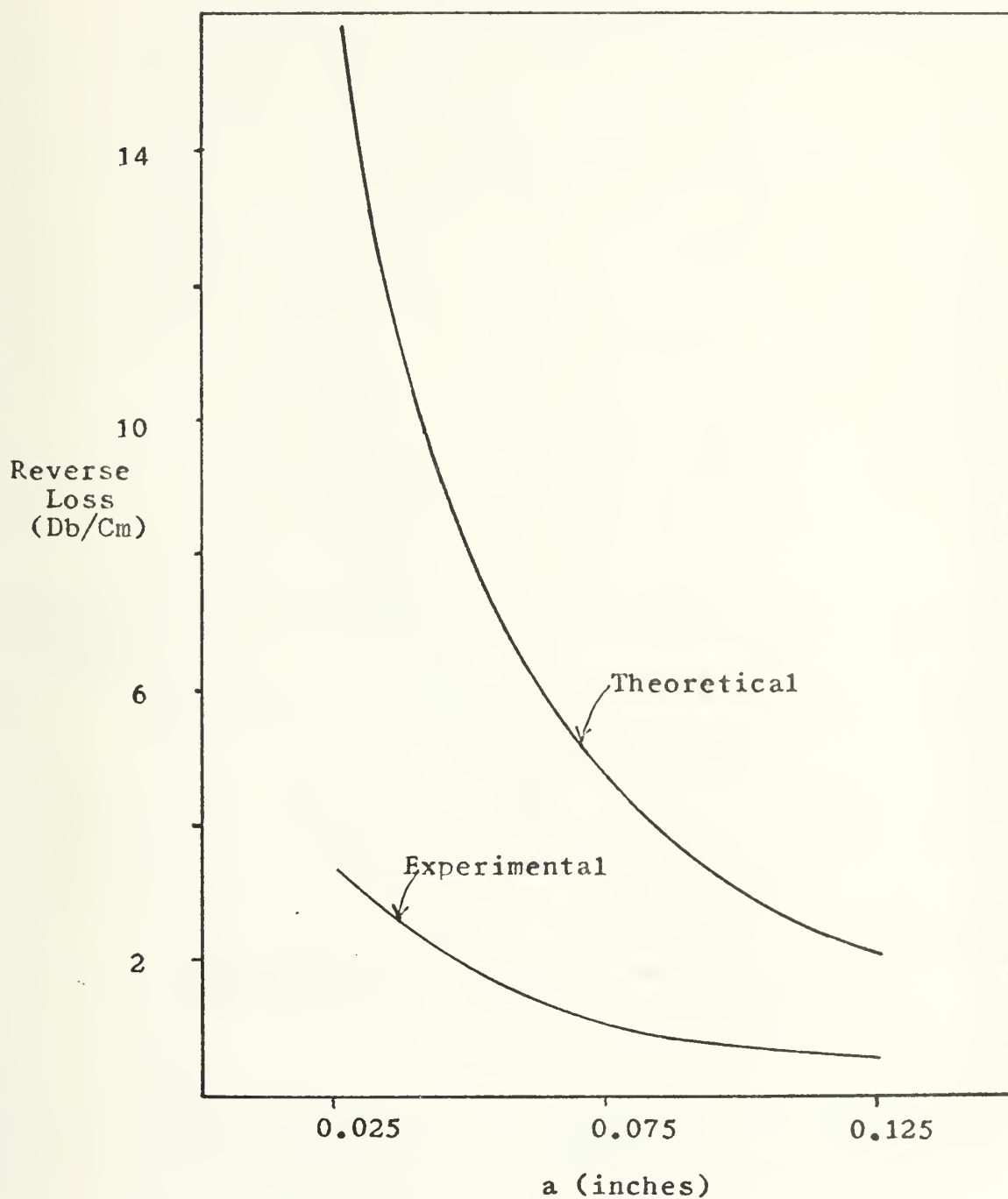


Figure 15. Theoretical and experimental values of reverse loss at the center frequency as a function of distance from the center of the slot for Garnet.

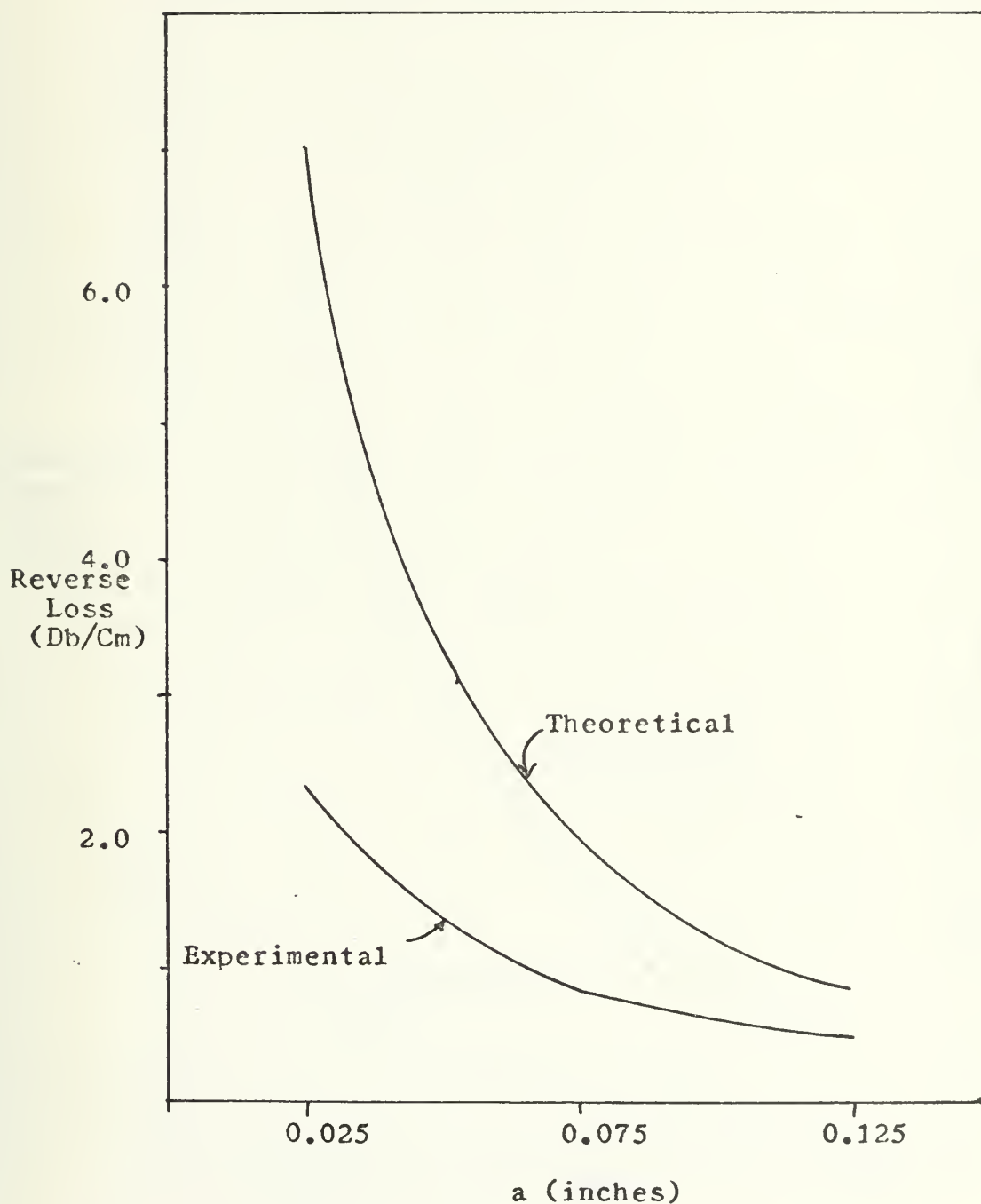


Figure 16. Theoretical and experimental values of reverse loss at the center frequency as a function of distance from the center of the slot for Spinel.

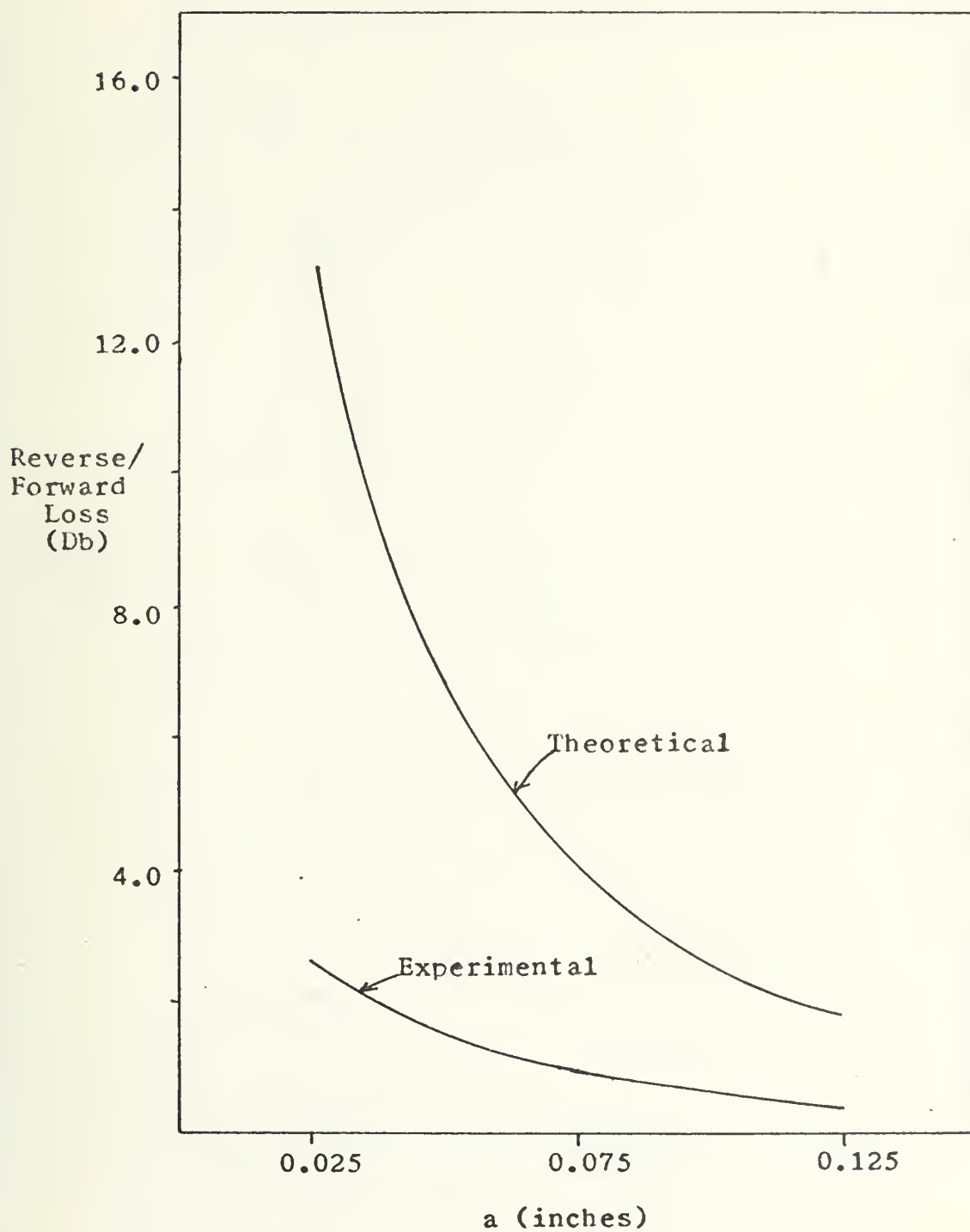


Figure 17. Ratio of reverse to forward attenuation at the center frequency as a function of distance from the center of the slot for Garnet.

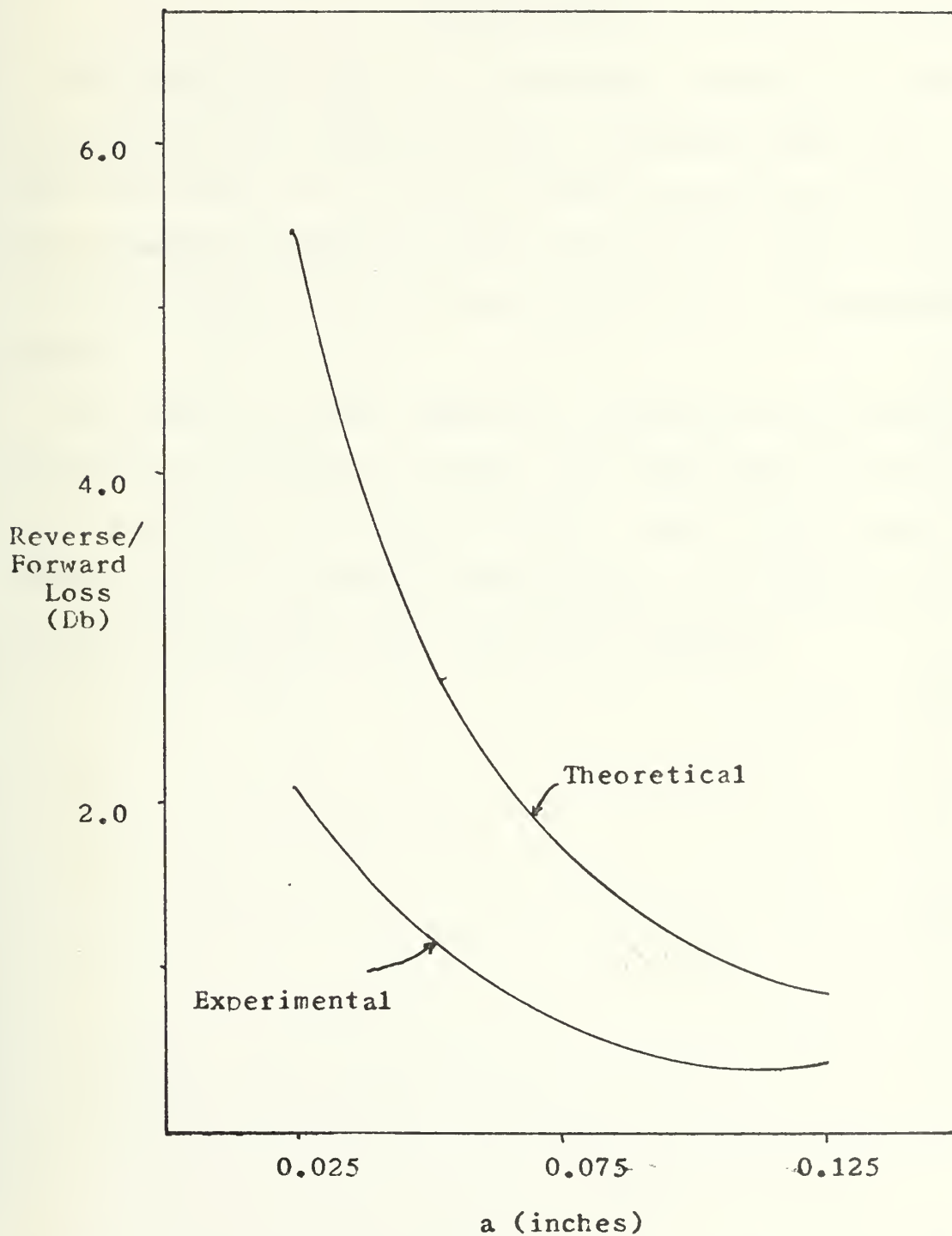


Figure 18. Ratio of reverse to forward attenuation at center frequency as a function of distance from the center of the slot for Spinel.

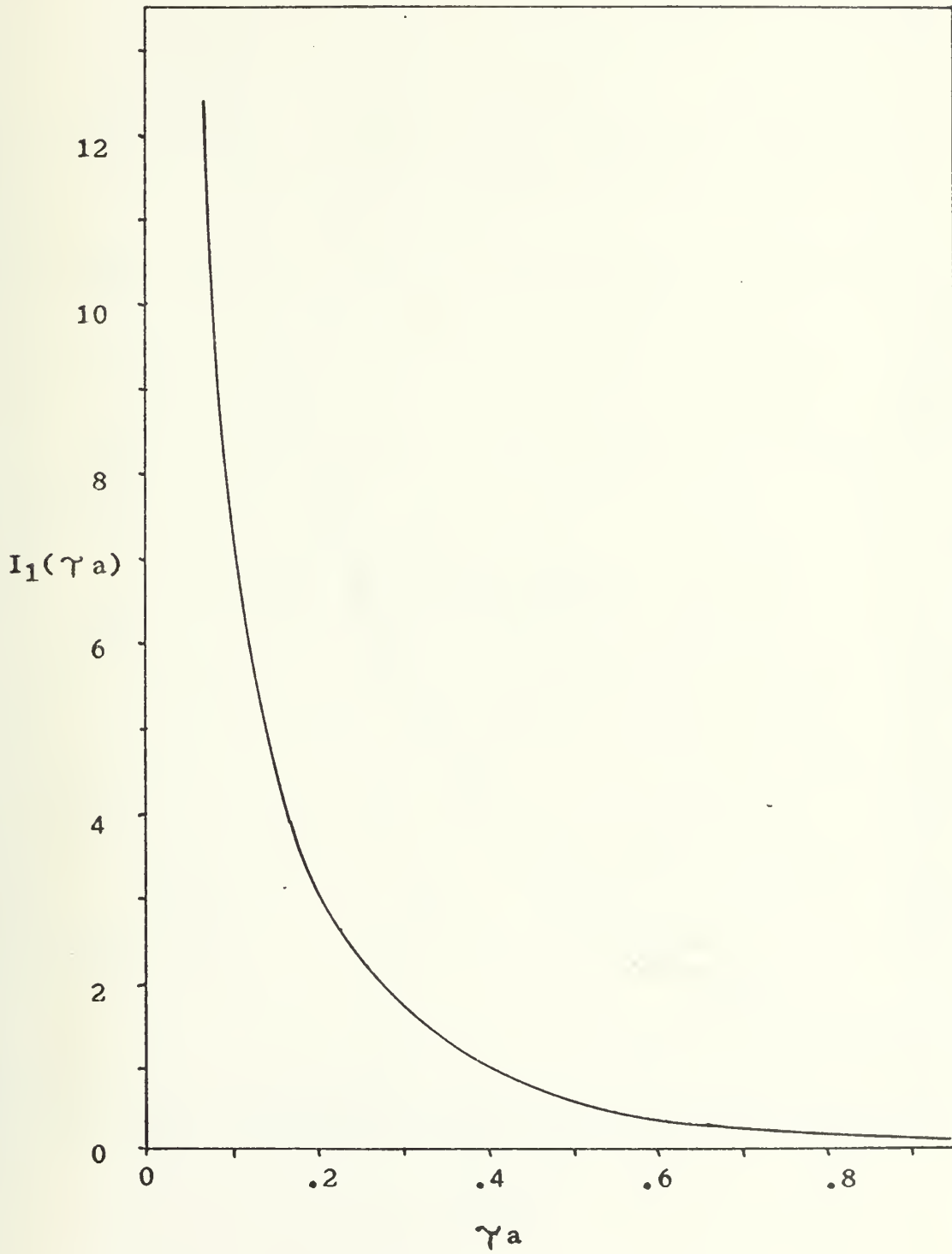
V. CONCLUSIONS

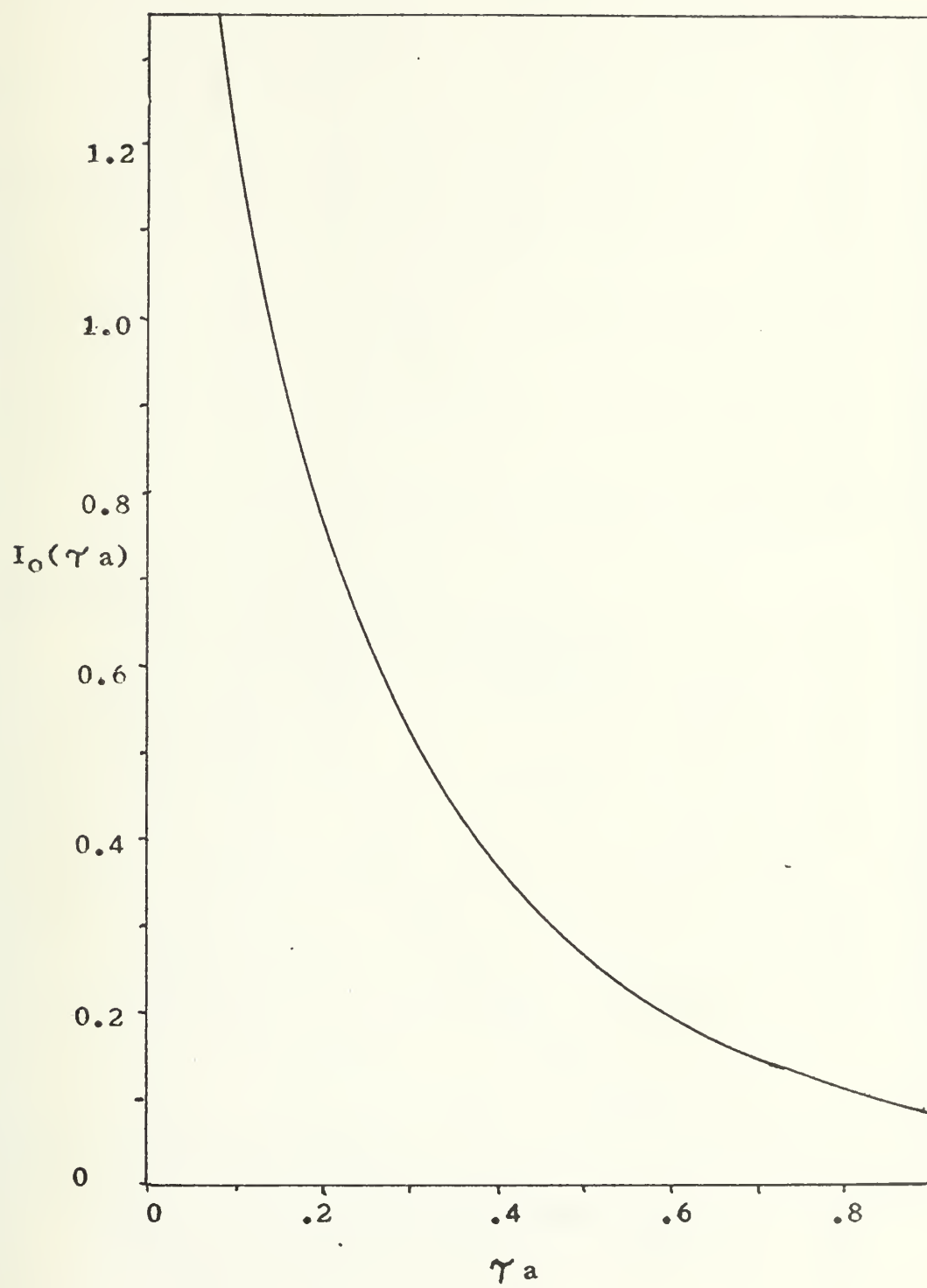
The theoretical and the experimental results of a slot line isolator have been presented. Although theory and experiment were not in accord as far as quantitative data was concerned, it appears evident that theory can be used to predict the behavior of the isolator for the configuration tested.

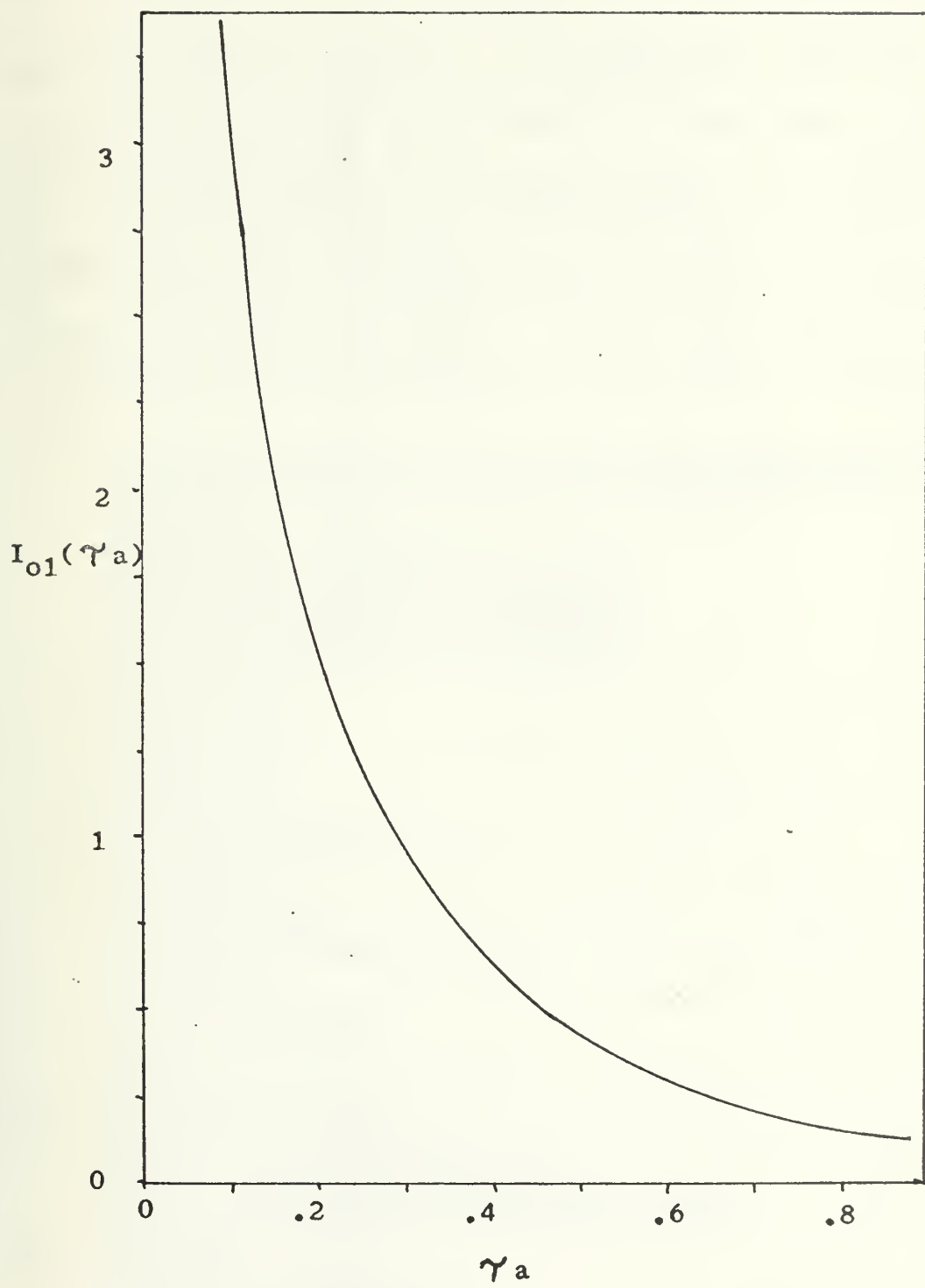
The results of this thesis have shown that non-reciprocal propagation can occur on a slot line loaded with a ferrite in the presence of a magnetic field. This initial success demonstrates that further investigation could define the optimum configuration for a slot line isolator.

APPENDIX A

Results of intergration of modified Bessel functions for small values of γa .







COMPUTER PROGRAM

THE IMAGINARY PARTS OF THE SUSCEPTIBILITY TENSOR AND THE FORWARD AND REVERSE ATTENUATION ARE EVALUATED FOR A SLOT LINE ISOLATOR OPERATING FROM 2.0GHZ TO 4.0GHZ. THE FOLLOWING DATA CARDS ARE REQUIRED.

- 1) FOUR PI MS COL. 1 TO 15, LINE WIDTH COL. 16 TO 30, THICKNESS COL. 31 TO 45.
- 2) SLOTTINE WAVE LENGTH FROM REF.(7). 2.0GHZ COL. 1 TO 15, 2.25GHZ COL. 16 TO 30, ECT.
- 3) SLOT LINE IMPEDANCE AVAILABLE FROM REF. (7). 2.0GHZ COL. 1 TO 15, 2.25GHZ COL. 16 TO 30, ECT.
- 4) IO(TAO A) FROM APPENDIX (A). 2.0GHZ COL. 1 TO 15, 2.25GHZ COL. 16 TO 30, ECT.
- 5) I1(TAO A) FROM APPENDIX(A). 2.0GHZ COL. 1 TO 15, 2.25GHZ COL. 15 TO 30, ECT.
- 6) IO1(TAO A) FROM APPENDIX(A). 2.0GHZ COL. 1 TO 15, 2.25GHZ COL. 16 TO 30, ECT.

```

    DIMENSION ALAMPR(50),ZZERO(50),FORWAR(50),REVERS(50),
    1FREQ(50),AFREQ(50),X(50),AKDPRI(50),AXDPRI(50),
    2AIO1A(50),ALAMBD(10),AIOA(50),AIIA(50)
    NUMBER=9
    READ(5,105) PIMS,DELH,THICK
    READ(5,110)(ALAMPR(I),I=1,NUMBER)
    READ(5,115)(ZZERO(I),I=1,NUMBER)
    READ(5,116)(AIOA(I),I=1,NUMBER)
    READ(5,117)(AIIA(I),I=1,NUMBER)
    READ(5,118)(AIO1A(I),I=1,NUMBER)
    SPEED=2.997E10
    ETA=3.767E2
    TFREQ=2.0E9
    FZERO=3.0E9
    CONS2=-2.0E0
    CONS4=4.0E0
    GYRO=2.8E6
    FSAT=GYRO*PIMS
    DELTAH=(GYRO*DELH)/2.0
    AAA=FZERO**2
    BBB=FSAT**2
    BBBB=FSAT*DELTAH
    CCC=DELTAH**2
    DDD=CONS2*FZERO*DELTAH*FSAT
    EEE=AAA-CCC
    GGG=AAA+CCC
    FFF=CONS4*CCC*AAA
    DO 20 I=1,NUMBER
    AK=I-1
    FREQ(I)=TFREQ+AK*0.25E9
    CONTINUE
    DO 100 I=1,NUMBER
    AFREQ(I)=(FREQ(I))**2
    DENOM=(EEE-AFREQ(I))**2+FFF
    AKDPRI(I)=(DDD*FREQ(I))/DENOM
    AXDPRI(I)=(BBBB*(GGG+AFREQ(I)))/DENOM
    X(I)=FZERO/FREQ(I)
    CONTINUE
    DO 220 I=1,NUMBER
    ALAMBD(I)=SPEED/FREQ(I)
    BETA=ZZERO(I)/ETA
    ALPHA=THICK/ALAMBD(I)
    THETB=ALAMBD(I)/ALAMPR(I)
    THETA=(ALAMBD(I)/ALAMPR(I))**2
    RHO=THETA-1.0

```



```

ALPHA1=2.0*BETA*ALPHA*AXDPRI(I)*((RHO**1.5)*AIOA(I)+AI
11A(I)*(THETB**2)*SQRT(RHO))/ALAMBD(I)
ALPHA2=(BETA*ALPHA*4.0*AKDPRI(I)*THETB*RHO*AI01A(I))/A
1LAMBD(I)
FCRWAR(I)=20*ALOG10(EXP(ALPHA1+ALPHA2))
REVERS(I)=20*ALOG10(EXP(ALPHA1-ALPHA2))
220 CONTINUE
WRITE(6,170)(AKDPRI(I),I=1,NUMBER)
WRITE(6,180)(AXDPRI(I),I=1,NUMBER)
WRITE(6,190)(FORWAR(I),I=1,NUMBER)
WRITE(6,200)(REVERS(I),I=1,NUMBER)
105 FORMAT(3F15.7)
110 FORMAT(5F15.7)
115 FORMAT(5F15.7)
116 FORMAT(5F15.7)
117 FORMAT(5F15.7)
118 FORMAT(5F15.7)
170 FORMAT('1',10X,'XSUBXY DOUBLE PRIME'///('0',E16.7))
180 FORMAT('1',10X,'XSUBXX DOUBLE PRIME'///('0',E16.7))
190 FORMAT('1',10X,'FORWARD LOSS IN DB/CM IS'///('0',E16.7
1))
200 FORMAT('1',10X,'REVERSE LOSS IN DB/CM IS'///('0',E16.7
1))
STOP
END

```


LIST OF REFERENCES

1. Cohn, S.B., "Slot Line on a Dielectric Substrate," IEEE Trans. Microwave Theory and Techniques, v. MTT-17, p. 768-778, October 1969.
2. Hines, M.E., "Reciprocal and Nonreciprocal Modes of Propagation in Ferrite Stripline and Microstrip Devices," IEEE Trans. Microwave Theory and Techniques, v. MTT-19, p. 442-451, May 1971.
3. Soohoo, R.F., Theory and Application of Ferrites, p. 59-76, Prentice-Hall, 1960.
4. Helszajn, J., Microwave Ferrite Engineering, Wiley-Interscience, 1969.
5. Mariani, E.A., Heinzman, C.P., Agrios, J.P., and Cohn, S.B., "Slot Line Characteristics," IEEE Trans. Microwave Theory and Techniques, v. MTT-17, p. 1091-1096, December 1969.
6. Knorr, J.B., "Perturbation Theory as Applied to an Open Boundary Structure Supporting Bound Waves," Unpublished.
7. United States Army Electronics Command, Contract DAAB07-68-C-0088, Microwave Synthesis Techniques Final Report, by E.G. Cristal, R.Y.C. Ho, D.K. Adams, S.B. Chon, L.A. Robinson, p. 38, November 1969.
8. Knorr, J.B., Slot Line Isolator Analysis, Unpublished.
9. System/360 Scientific Subroutine Package, H20-0205-3, Programmer's Manual.

INITIAL DISTRIBUTION LIST

	No. Copies
1. Defense Documentation Center Cameron Station Alexandria, Virginia	2
2. Library, Code 0212 Naval Postgraduate School Monterey, California 93940	2
3. Professor J.B. Knorr, Code 52KO Department of Electrical Engineering Naval Postgraduate School Monterey, California 93940	1
4. Lt. Imon L. Pilcher 1275 Spruance Road Monterey, California 93940	1

DOCUMENT CONTROL DATA - R & D

(Security classification of title, body of abstract and indexing annotation must be entered when the overall report is classified)

ORIGINATING ACTIVITY (Corporate author)

Naval Postgraduate School
Monterey, California 93940

2a. REPORT SECURITY CLASSIFICATION

Unclassified

2b. GROUP

REPORT TITLE

Slot Line Ferrite Isolator

DESCRIPTIVE NOTES (Type of report and, inclusive dates)

Master's Thesis; June 1973

AUTHOR(S) (First name, middle initial, last name)

Imon Lester Pilcher

REPORT DATE

June 1973

7a. TOTAL NO. OF PAGES

45

7b. NO. OF REFS

9

CONTRACT OR GRANT NO.

9a. ORIGINATOR'S REPORT NUMBER(S)

PROJECT NO.

9b. OTHER REPORT NO(S) (Any other numbers that may be assigned this report)

DISTRIBUTION STATEMENT

Approved for public release; distribution unlimited.

SUPPLEMENTARY NOTES

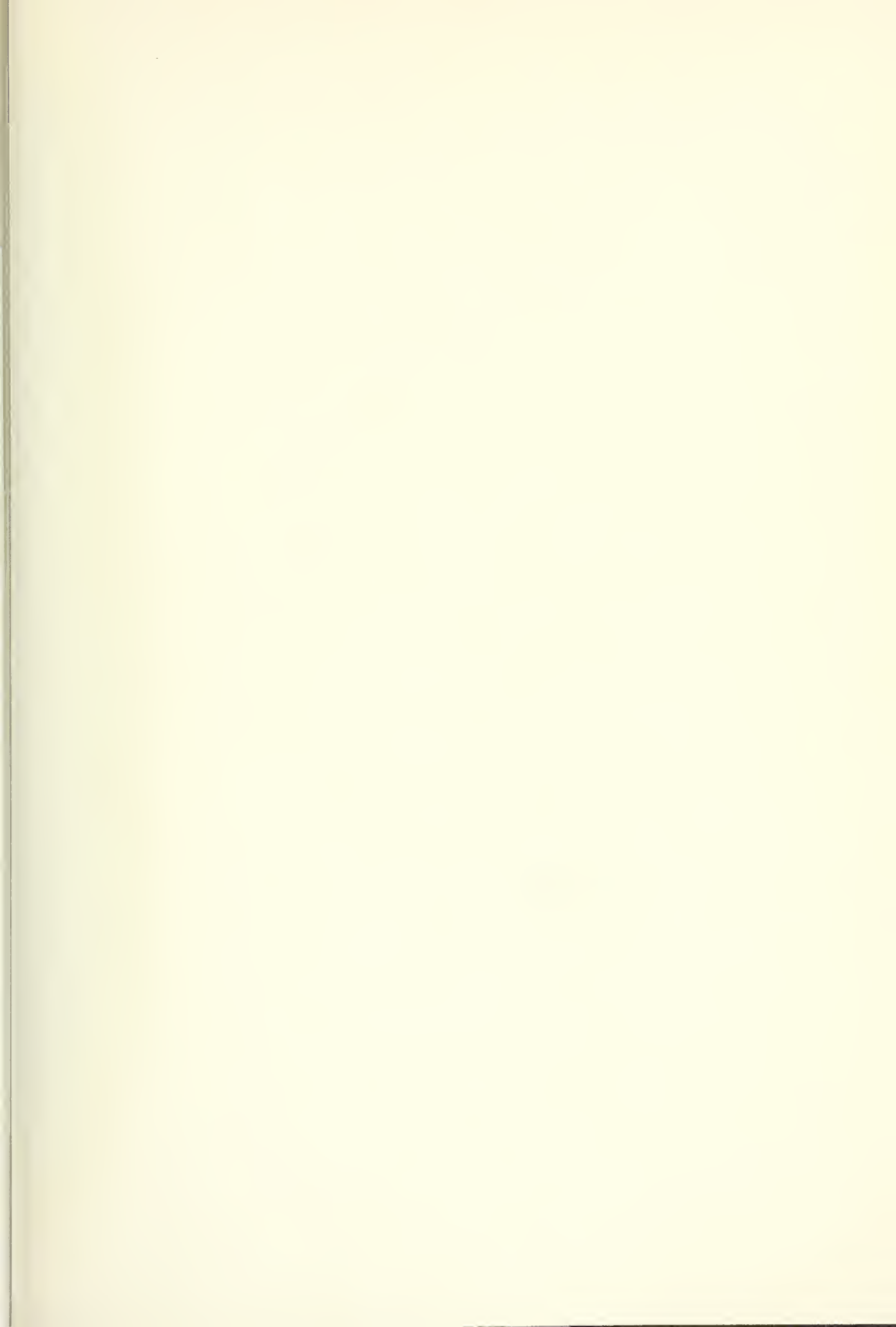
12. SPONSORING MILITARY ACTIVITY

Naval Postgraduate School
Monterey, California 93940

ABSTRACT

A slot line isolator configuration is investigated experimentally. The configuration is analyzed using perturbation theory. Theoretical results obtained from a computer program based on the analysis are compared with the experimental measurements.

KEY WORDS	LINK A		LINK B		LINK C	
	ROLE	WT	ROLE	WT	ROLE	WT
Slot Line Isolator						



Thesis
P5415 Pilcher 145225
c.1 Slot line ferrite
isolator.

Thesis
P5415 Pilcher 145226
c.1 Slot line ferrite
isolator.



3 2768 000 99317 4
DUDLEY KNOX LIBRARY